# He scattering from substitutionally disordered mixed monolayers: Experimental and theoretical studies of Xe+Kr on Pt(111)

M. Yanuka and A. T. Yinnon
*Department of Physical Chemistry and The Fritz Haber Research Center for Molecular Dynamics, The Hebrew University, Jerusalem 91904, Israel*

R. B. Gerber
*Department of Physical Chemistry and The Fritz Haber Research Center for Molecular Dynamics, The Hebrew University, Jerusalem 91904, Israel and Department of Chemistry University of California, Irvine, California 92717*

P. Zeppenfeld, K. Kern,[a] U. Becher, and G. Comsa
*IGV, KFA-Forschungszentrum Jülich, Postfach 1913, D-5170, Jülich, Germany*

(Received 18 May 1993; accepted 23 July 1993)

The diffraction of thermal He atoms from mixed Xe+Kr monolayers on Pt(111) was measured, and the results were compared with theoretical studies of these systems. The results shed light on the structural properties of these disordered systems, and on their relation to the He diffraction intensities. Experimentally, the specular (0,0), the (1,0), and the (2,0) Bragg peak intensities were measured for monolayers of different Kr:Xe concentration ratios. The theoretical calculations included Monte Carlo simulations of the mixed disordered monolayers, and quantum calculations in the Sudden approximation of the scattering intensities from the simulated disordered structures. The following main results were obtained: (1) Both experiment and the Monte Carlo simulations suggest that the mixed Xe+Kr monolayers are periodic for all Xe:Kr concentration ratios, the lattice constant varies linearly with the Xe:Kr ratio. The domain size of the 2D crystals, from experiment and theory, is found to be larger than 100 Å. (2) The Monte Carlo simulations suggest that the Xe+Kr monolayers form an almost ideal substitutionally disordered lattice. (3) Using a semiempirical Debye–Waller factor, reasonable agreement is found between the theoretical and the measured diffraction intensities, thus supporting the calculated structural model for the disordered surface. (4) The theoretical scattering calculations show that in addition to the diffraction peaks, there are also intensity maxima at non-Bragg positions. These are entirely due to the lattice disorder, and are identified as a recently found new type of Rainbow effect that can furnish important information on disordered surfaces. The results demonstrate the power of He scattering as a tool for exploring substitutionally disordered surfaces.

## I. INTRODUCTION

The structure of physisorbed monolayers is a central topic in surface crystallography, and has received extensive experimental and theoretical attention over the years. In this framework, there is special conceptual interest in the study of rare-gas monolayers, since the adsorbates are spherical, and the interactions between them are well known, which are major advantages for efforts at rigorous, first-principles, theoretical understanding of the structure. These systems have thus been the subject of detailed theoretical calculations,[1] and also of extensive experimental studies using, among other techniques, diffractive scattering of He atoms from the crystalline monolayers.[2–4] As a consequence, good quantitative understanding is at hand on the structure and vibrational dynamics of several rare-gas monolayer and multilayer systems on metal surfaces such as Ag(111) and Pt(111), on graphite C(0001), and on other supporting surfaces.[1–4] On the other hand, relatively little is known on the structure of mixed monolayers of two different rare gases. The conceptual issue is a very important one, since such mixed monolayers represent two-dimensional disordered systems where the interactions between the particles are well known, thus providing a natural testing ground for theoretical models and simulations of such disordered phases. The objective of the present article is indeed to explore the structure of mixed xenon and krypton monolayers on the relatively smooth Pt(111) surface. The aim is to understand the crystallography of these disordered systems at the atomic level, to shed light on the precise nature of the disorder involved, and to establish whether first-principles theoretical calculations, with the presently available interaction potentials, can provide an adequate description, compatible with experiment. The study presented here consists mainly of three components: (i) Theoretical Monte Carlo simulations of the structure and other properties, of the mixed rare gas: As will be shown, the Xe+Kr monolayers are found to be substitutionally disordered, but crystalline periodic over the entire range of the Xe:Kr concentration ratios at the conditions of this study. (ii) He scattering experiments, with measurements of the Bragg diffraction peak intensities: As is intuitively expected, and as found in

[a]Present address: Institut de Physique Expérimentale EPF Lausanne, CH-1015 Ecublens, Switzerland.

 0021-9606/93/99(10)/8280/10/$6.00 

theoretical scattering calculations,[5] substitutionally disordered, periodic crystalline surfaces give rise to sharply defined Bragg diffraction peaks (although the calculations show also other intensity maxima for such systems[5]). (iii) Calculations of He scattering from the simulated structures of the mixed monolayers: The calculated diffraction intensities are compared with experiment, thus lending support for the calculated microscopic structure.

Thermal He scattering has great advantages as a tool for exploring the soft physisorbed monolayers studied here. It is nondestructive, and the scattered particles *only* probe the outermost layer.[6–8] At the same time, the present article seeks also to investigate the utility of He scattering as a tool for exploring substitutional disorder on surfaces. In general, structurally disordered surfaces do not necessarily give rise to Bragg diffraction, but this depends upon the type and extent of the disorder. Disordered surfaces which do not give rise to measurable Bragg diffraction peaks can still be explored by He scattering. A very general and powerful approach is the one that studies the attenuation of the specular reflection of He from the surface due to defects or other disorders.[9] Also, in the case of certain isolated defects on smooth metal surfaces, e.g., CO adsorbates on Pt(111), non-Bragg maxima in the angular scattering intensity distribution of the scattered He were measured, and used to throw light on the microstructure of the defect.[10,11] Indeed, so far Bragg diffraction studies of structural disorder on surfaces were limited to low-concentration defects in otherwise ordered crystalline surfaces,[12] in which case the width of the Bragg peaks depends upon the defect concentration. For periodic, substitutionally disordered surfaces, pronounced Bragg diffraction peaks occur and it seems natural to explore these features in order to extract the microscopic structure of the disordered system. Our combined experimental–theoretical study will pursue the questions of (i) how much can be learned on the detailed microscopic structure from the Bragg peaks; (ii) how the Bragg peaks can be treated theoretically for such disordered systems, and (iii) what other features exist in the diffraction signature of the mixed monolayers.

The structure of the article is as follows: Sec. II describes the systems studied, and outlines the methods used and the assumptions made in the theoretical part of this work. Section III presents an account of the main results obtained both theoretically and experimentally, with an analysis both of the structures of the systems studied and the properties of the He scattering from the substitutionally disordered monolayer. Concluding remarks are presented in Sec. IV.

## II. SYSTEMS AND METHODS

The systems investigated in this study are mixed monolayers of Xe and Kr on Pt(111). Both theory and experiment cover monolayers with different Xe:Kr concentration ratios, ranging from pure Xe to pure Kr monolayers. The study is carried out for conditions in which the monolayers are incommensurate with the supporting surface.

### A. Theoretical methods

#### 1. Monte Carlo simulations of structure

In modeling the substrate, we assumed a flat supporting surface. Indeed, the Pt(111) surface is a relatively smooth one, and it appears a reasonable approximation to assume that for the incommensurate monolayers the role of the underlying surface structure is small, and can be neglected. For the interaction between the monolayer and the Pt support, a sum over pairwise interactions between each rare gas atom and the metal surface was taken:

$$V_{M-S}=\sum_i V_{\alpha(i)}(z_i), \tag{1}$$

where $z_i$ is the distance of the rare-gas atom $i$ from the Pt surface plane, and $\alpha(i)$ is a label for the identity of atom $i$ (either Xe or Kr). At the time the research was carried out the most accurate potential between a Xe atom and Pt(111) was the empirical potential of Black,[13] which we employed. Very recently an improved potential was developed by Barker and Rettner.[14] We fitted a simple Lennard-Jones potential to the Black potential function (over the range of configurations pertinent to the present study). The fitted Xe atom/Pt surface potential has a well depth of 0.480 eV, and an equilibrium distance from a surface reference plane of 3.00 Å. Gibson and Sibener[4] obtained Xe/Ag surface and Kr/Ag surface potentials by fitting their experimental data. Assuming that the ratio between the well depths for Xe/Pt(111) and Kr/Pt(111) is the same as that of Xe/Ag(111) and Kr/Ag(111), we obtain a Kr/Pt(111) well depth of 0.300 eV. This well depth as well as that of Xe/Pt(111) are higher than those obtained recently from experiment,[3] 0.128 and 0.280 eV, respectively, and from theory.[14] However, we found the height of the well depths to have little influence on our qualitative results. In contrast, the difference between the equilibrium distances of Xe and Kr from the Pt(111) surface plane plays a significant role in the systems studied. Unfortunately, little is known on this, since there is no experimental data bearing on this issue. We used two very different choices for $z_{\min}(\mathrm{Xe})-z_{\min}(\mathrm{Kr})$: (1) Determination of this difference from the Gibson and Sibener Xe/silver and Kr/silver potentials,[4] scaling the distances for the case of Pt(111). This gave $z_{\min}(\mathrm{Xe})-z_{\min}(\mathrm{Kr})=-0.17$ Å, i.e., the equilibrium distance of Kr is farther from the surface plane than that of Xe. (2) Determination of the difference based on the different sizes of the rare-gas atoms. This gives $z_{\min}(\mathrm{Xe})-z_{\min}(\mathrm{Kr})=0.233$ Å. The Lennard-Jones rare-gas/Pt potentials corresponding to each of the two choices were used in the Monte Carlo simulations. The different structures and the calculated scattering intensities obtained using the two different potentials are discussed later and compared to the experiment. For the potential energy of the monolayer itself, we use a pairwise sum of atom–atom interactions, i.e.,

$$V_M=\sum_i \sum_{j<i} U_{\alpha(i),\alpha(j)}(r_{ij}), \tag{2}$$

where $r_{ij}$ is the distance between the rare-gas atoms $i$ and $j$, and $\alpha(i)$ labels the identity of atom $i$. We used gas-phase Lennard-Jones potentials for the Xe–Xe, Xe–Kr, and Kr–Kr interactions.[15] This simplifies the computational effort in the Monte Carlo simulations reported later, but is certainly a very approximate level of treatment. The best available gas-phase potentials are considerably superior in accuracy to the LJ interactions, and the neglect of three-body interactions, as well as that of metal-mediated forces between the rare-gas atoms, may also be quantitatively significant. We propose to use more refined potentials in future investigations, when more extensive evidence from experiment and theory becomes available to find the direction where improvements are necessary.

The total potential function of the monolayer system is

$$U=V_M+V_{M-S}. \tag{3}$$

The Monte Carlo simulations were carried out using a standard Metropolis algorithm.[16] In this algorithm, a repetitive random sampling of configurations is carried out as follows: Given a configuration of the $N$ atom system $\mathbf{r}\equiv\{\mathbf{r}_1,...,\mathbf{r}_N\}$ a successive configuration $\mathbf{r}'$ is generated by a random shift of a randomly picked atom:

$$\mathbf{r}_i=(x_i,y_i,z_i)\rightarrow\mathbf{r}_i'=(x_i+\eta_x\Delta x,y_i+\eta_y\Delta y,z_i+\eta_z\Delta z), \tag{4}$$

where $\eta_x,\eta_y,\eta_z$ are random numbers between 0 and 1, and $\Delta x,\Delta y,\Delta z$ represent displacement constants for the three coordinates. The new configuration $\mathbf{r}'=\{\mathbf{r}_1,...,\mathbf{r}_i',...,\mathbf{r}_N\}$ is accepted if at last one of the following conditions is satisfied:

$$\Delta U\equiv U(\mathbf{r}')-U(\mathbf{r})<0 \tag{5a}$$

or

$$\exp\left[-\frac{\Delta U}{k_BT}\right]>\xi, \tag{5b}$$

where $\xi$ is a random number between 0 and 1. The process continues by repeating the procedure until, in principle, the entire relevant configuration space is sampled. The magnitudes of displacement constants $\Delta x,\Delta y,\Delta z$ are chosen so as to accelerate convergence. From the results one can readily generate average thermodynamic and structural properties such as the average structure, the mean interaction potential, the free energy, etc. Our simulations began above the segregation temperature of Xe and Kr. We estimated this temperature to lie around 16 K. We started with a $50\times50$ hexagonal lattice array, but several calculations were carried out for larger systems and convergence of the results with respect to cluster size was tested and confirmed. The calculations were carried out for large open clusters, rather than with periodic boundary conditions, since the latter may favor periodic crystalline structures. In order to eliminate the potential difficulty of getting trapped in local minima, a simulated annealing procedure was employed. Starting with a lattice structure as mentioned above, the temperature was raised to a high value $T_1$, where the system explores sufficiently large regions of configuration space. The system was then cooled gradually to the temperature of interest $T$. For example, to simulate the monolayers at $T=40$ K, we annealed the system by first simulating at $T=40$ K, then heating to $T_1=100$ K, and then finally cooling back gradually to $T=40$ K. (100 K is above the boiling temperature of Kr, but the computer annealing time used here was too short for any boiling to occur.)

From the Monte Carlo simulations we calculated for the monolayers with various Xe:Kr ratio properties such as the average structure, the radical pair distribution functions, angular distribution functions, the Helmholtz free energy, etc. The results will be described in the next section. The distribution of structures obtained for each given monolayer at the temperature of interest was used as input for the He scattering calculations.

### 2. He scattering calculations

The calculations carried out in this study are for He scattering from rigid, nonvibrating structures. This approximate treatment is generally adopted for calculations of He scattering from ordered crystalline structures,[8,17] e.g., in the case closely related to the present study of He diffraction from ordered monolayers of Xe on graphite.[18] To account for the attenuation of the diffraction peak intensities due to surface vibrations, Debye–Waller factors are applied to the static-surface theoretical results, and while this involves some approximations[19,20] there is reasonable evidence for the validity of this approach in most cases.[17] It should be recognized that the rigid-surface treatment, with subsequent Debye–Waller corrections neglects the influence of coherent and incoherent inelastic phonon scattering on the *dynamics* of the coherent elastic scattering.[19,20] We tentatively justify this treatment on the basis of evidence from comparisons with experiment for ordered crystalline systems. For disordered systems, however, coherent elastic scattering is by no means confined to Bragg diffraction.[5] Indeed, it will be shown later that intensity maxima at non-Bragg angles occur for the monolayers studied here. The calculations of the angular intensity distribution for scattering from disordered surfaces is considerably more difficult than that for ordered, periodic structures.[21] Several approaches mostly based on various approximations and specific models, have been proposed.[22–27] In principle, numerically exact calculations of He scattering from static (nonvibrating) disordered surfaces can be carried out by efficient grid methods for solving the time-dependent Schrödinger equation[28] as was demonstrated for models of structurally disordered surfaces, including a one-dimensional mixed "surface."[29,30] However, for the realistic systems studied here the required computational effort is very great, since the description of the disordered structures requires very large grids. The scattering calculations from the simulated disordered structures reported here were therefore carried out in the framework of the Sudden approximation.[24,28] This method, first used by some of the present authors for He diffraction from ordered crystalline surfaces,[28] was applied extensively to scattering from disordered surfaces, including isolated defects in otherwise crystalline ordered surfaces, and models of e.g. substitutionally disordered surfaces.[29,31,5] On the

basis of the experience gained with the Sudden approximation, including particular tests against numerically exact calculations for several model systems,[28,29,31] we estimate that at least the main predictions of the Sudden calculations should be reliable for the systems considered here. The Sudden approximation takes the following form for the systems studied below. Consider a particular (static) configuration $\mathbf{r}$ of a disordered monolayer system. $\mathbf{r}$ denotes, as previously in this section, the positions of the $N$ Xe and Kr atoms. The angular intensity distribution for the He scattered from the monolayer involves an average over all configurations pertinent to the given temperature and surface density:[24]

$$I(\mathbf{k}\rightarrow\mathbf{k}')=\left\langle\left|\frac{1}{A}\int\int e^{i\Delta\mathbf{K}\cdot\mathbf{R}}e^{2i\eta_r(\mathbf{R})}\,d\mathbf{R}\right|^2\right\rangle_r . \tag{6}$$

In this expression $\hbar\mathbf{k}$ is the incident momentum, and $\hbar\mathbf{k}'$ the final momentum of the He atoms; $\hbar\Delta\mathbf{K}=\hbar\mathbf{k}'-\hbar\mathbf{k}$ is the momentum transfer of the He parallel to the surface; $\mathbf{R}\equiv(x,y)$ denotes the coordinates of the He atom along the plane of the surface, $A$ is the area of the surface, and the $\mathbf{R}$ integration in (6) is over that area; $\langle\cdots\rangle_r$ denotes the average over all configurations (at the given temperature and surface density) of the quantity in parenthesis, and $\eta_r(\mathbf{R})$ denotes the phase shift for He scattering for a monolayer having a configuration $\mathbf{r}$, and when the He has a position $\mathbf{R}$ along the surface. $\eta_r(\mathbf{R})$ is given by

$$\eta_r(\mathbf{R})=\int_{z_R}^{\infty}dz\{[k_z^2-2mV_r(\mathbf{R},z)/\hbar^2]^{1/2}-k_z\}-k_z z_R , \tag{7}$$

where $m$ is the mass of the He atom, $\hbar k_z$ is the incident momentum of the atom normal to the surface, $z$ denotes the distance of the He atom from the surface plane, and $V_r(\mathbf{R},z)\equiv V_r(x,y,z)$ is the interaction potential between the He atom, at position $\rho=(x,y,z)$, and the surface, having the static configuration $\mathbf{r}$. $z_R$ in Eq. (7) denotes the classical turning point for the He when colliding with the surface at the lateral position $\mathbf{R}=(x,y)$, i.e., $z_R$ is the $z$ value for which

$$\hbar^2k_z^2-2mV_r(\mathbf{R},z)=0. \tag{8}$$

The interaction potential $V_r(x,y,z)$ between the He atom and the mixed Xe+Kr monolayer at configuration $\mathbf{r}=\{\mathbf{r}_1,\ldots,\mathbf{r}_N\}$ of the monolayer atoms, was obtained as a sum of He/Xe and He/Kr pair potentials:

$$\mathbf{V}_r(\rho)=\sum_i W_{\alpha(i)}(\rho-\mathbf{r}_i), \tag{9}$$

where $\alpha(i)$ indicates the identity of the monolayer atom $i$. The He/Xe and He/Kr pair potentials were taken from gas-phase scattering data.[15] The evaluation of the intensity expression (6) requires therefore calculation of the scattering from each configuration $\mathbf{r}$ of the disordered monolayer that contributes significantly at the temperature considered, and the evaluation of the average over the various configurations using the Monte Carlo simulation results. In comparing the calculated scattering intensities for the rigid monolayer with the experimental data, we shall assume a Debye–Waller type of attenuation, i.e.,

$$I_T(\mathbf{k}\rightarrow\mathbf{k}')=F_{\mathbf{k},\mathbf{k}'}I(\mathbf{k}\rightarrow\mathbf{k}'), \tag{10}$$

where $I_T(\mathbf{k}\rightarrow\mathbf{k}')$ is the experimental scattering intensity for a (vibrating) surface at temperature $T$, and $I$ is the rigid-surface intensity, calculated from Eq. (6). To our knowledge, the theory of Debye–Waller attenuation of He scattering from a disordered surface of the type considered here has not been developed yet. In this study we adopt a semiempirical approach, and assume

$$F_{k,k'}=C_1F_{k,k'}^{(1)}+C_2F_{k,k'}^{(2)}, \tag{11}$$

where $F_{k,k'}^{(1)},F_{k,k'}^{(2)}$ are interpreted as DW-type attenuation factors for the pure Xe and the pure Kr monolayer, respectively, and $C_1,C_2$ are the relative concentrations of Xe and of Kr, $C_1+C_2=1$. Values for $F_{k,k'}^{(1)}$ and $F_{k,k'}^{(2)}$ were chosen so as to get a best fit between the theoretical results and the experimental data. Comparison with experiment suggests that this is at least acceptable as a first approximation.

### B. Experimental methodology

The experimental setup used in the experiments is described in detail by David *et al.*[32] We briefly summarize its main characteristics: The supersonic beam is generated by expanding He gas from a pressure of about 150 bar through a small nozzle (5 $\mu$m in diameter). The resulting He beam is highly monochromatic ($\Delta E/E=1.4\%$). It is directed at the sample and the scattered He atoms are detected in a quadrupole mass spectrometer. The total scattering angle is fixed ($\theta_i+\theta_f=90°$) and the scattering conditions are varied by rotating the sample about an axis normal to the scattering plane yielding a parallel momentum transfer $Q=k_i[\sin(\theta_i)-\sin(\theta_f)]=\sqrt{2}k_i\sin(\theta_i-45°)$. The azimuthal orientation of the sample can be varied by rotating the crystal about its surface normal leaving the polar angle and wave vector transfer unchanged. The angular divergence of the incident beam and the angle subtended by the detector are both 0.2°. Together with the energy spread of the incident beam this results in a wave vector resolution of the apparatus of about 0.02 Å$^{-1}$. The sample temperature can be varied from 25 to 1500 K. The Pt(111) sample is a high quality surface with an average terrace width $\geqslant$2000 Å. It was cleaned by cycles of Ar sputtering and heating in oxygen until no traces of impurities could be detected by Auger spectroscopy. Before each experiment the sample was cleaned by sputtering with Ar and subsequent annealing at about 1000 K. The sample smoothness and cleanliness was routinely checked by monitoring the He reflectivity, which constitutes a sensitive probe for defects and impurities.[9]

The rare gases were adsorbed onto the Pt(111) substrate by exposing the sample to a partial pressure of the rare gas. The amount actually adsorbed on the surface (i.e., the coverage) can be accurately determined by monitoring the decrease of the He reflectivity as a function of exposure.[3,33] Once this coverage calibration is established

the desired rare gas coverage can be controlled within an estimated error of ±5% by dosing the appropriate amount. In the present case the two components Kr and Xe were adsorbed successively, first Kr followed by Xe. By monitoring the He reflectivity, it was checked that the presence of Kr does not modify (within the accuracy of our experiment) the adsorption properties of the Xe as compared to the adsorption of the clean Pt(111) surface: On the clean as well as on the Kr precovered Pt(111) surface the sticking probability for Xe is close to unity. In the following we will only discuss experimental results which were obtained from mixtures at about the same total coverage of 60% of a monolayer. In fact, close to monolayer completion both the Xe and Kr adlayer undergo structural phase transitions that would obscure the properties of the mixtures which are of interest here.

Once the two components are adsorbed on the surface the structure is investigated by taking polar and azimuthal diffraction scans yielding the size and orientation of the unit cell. If the rare gases are adsorbed at low surface temperature (≤25 K) separate Kr and Xe $n$th order diffraction peaks are observed along the $\overline{\Gamma K}$ azimuth of the Pt(111) substrate indicating the formation of two distinct hexagonal phases rotated by 30° with respect to the underlying substrate. The wave vector positions of the diffraction peaks are close to the positions found in the pure Kr and Xe phases which demonstrates that at these low temperatures Kr and Xe are still phase separated after successive adsorption. This, however, is attributed to the low mobility of the atoms rather than the thermodynamic stability of the unmixed phase. After annealing the system at about 35 K, only single $n$th order diffraction peaks along the $\overline{\Gamma K}$ azimuth were observed whose positions are located between those for the pure phases. As will be demonstrated later this single "intermediate" diffraction peak is characteristic for the complete random substitutionally mixed Xe+Kr phase. All the experimental results reported here were obtained from mixtures that were carefully annealed at about 40 K.

Figure 1 depicts a polar He diffraction scan from a 50% Xe:50% Kr mixture on Pt(111) showing the first and second order diffraction peaks. In the present context, the position and intensities of the first and second order diffraction peaks from mixtures of various composition ratio are evaluated. The results will be discussed together with the results of the Monte Carlo simulation in Sec. III. A detailed lineshape analysis of a large number of similar diffraction scans around the second order diffraction peak (2,0) (which happens to be the most intense) and taken at different total coverages is presented in Ref. 34.

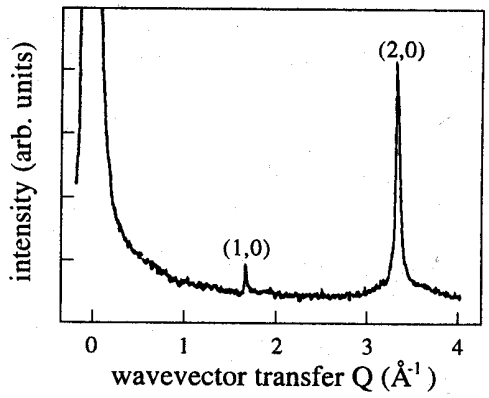


FIG. 1. He diffraction scan for a 50% Xe:50% Kr (total coverage $\theta_{Xe+Kr}$ =0.5 ML) binary mixture adsorbed on a Pt(111) substrate at $T$=40 K. The diffraction scan is characterized by relatively sharp Bragg diffraction peaks (1,0) and (2,0) at parallel wave vector transfer $Q$=1.68 Å$^{-1}$ and $Q$=3.36 Å$^{-1}$, respectively, indicating a highly crystalline ordered mixed phase exhibiting an "average" lattice parameter of 4.32 Å.

## III. RESULTS AND DISCUSSION

The main findings of this study can be grouped into the following topics.

### A. Periodicity of the structures

Both the Monte Carlo simulations and the experimental diffraction data show that the mixed monolayers form periodic surface structures over domains of the order of 100 Å at least. Periodic structures are obtained for monolayers of any Xe:Kr composition ratio. The Monte Carlo simulations predict periodic structures also for all composition ratios for both types of Xe/Pt(111), Kr/Pt(111) potentials used—the one that has Kr located nearer than Xe to the Pt surface plane, and the type that gives the opposite behavior (see Sec. II). The crystalline structures are hexagonal. They are clearly determined by the lateral interactions since theoretically and experimentally, the monolayer lattice constant varies with the Xe:Kr concentration ratio and theoretically a completely flat Pt(111) surface was assumed. Figure 2 shows the hexagonal lattice constant as a function of the fraction of Xe in the monolayer. In the experimental pronounced (1,0) and (2,0) Bragg diffraction peaks are observed (see Fig. 1), which confirms the lateral periodicity of the structures. The experimental lattice constant values shown in Fig. 2 were

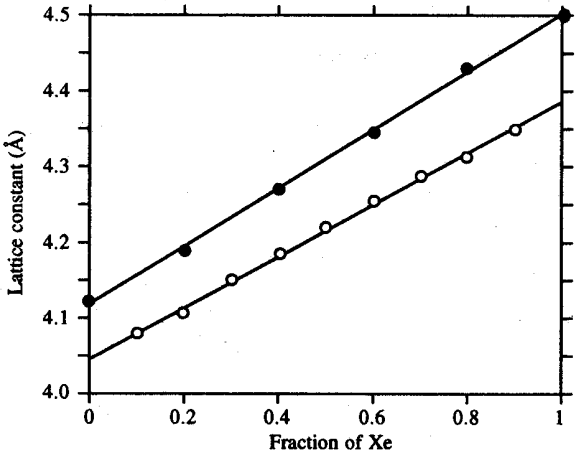


FIG. 2. The lattice constant as a function of the Xe fraction in the monolayer at $T$=40 K: Theory—open circles; experiment—full circles.

extracted from the measured diffraction angle of the Bragg peak positions. The theoretical lattice constant values in Fig. 2 are from the calculation using the Xe/Pt, Kr/Pt potentials which give the "lower Xe" geometry. The other type of potentials gives lateral lattice constants that differ only slightly. Both theory and experiment show a linear variation of the lattice constant with the Xe:Kr ratio—a "Vegard Law" type of behavior.[35] The agreement between the theoretical and the experimental results is very good, as far as the linear dependence upon the mixing ratio is concerned. However, the the theoretical and absolute values for the experimental lattice constant values for a given Kr:Xe ratio differ by a few percent only. This is almost certainly due to the insufficient accuracy of the potential functions used. It is possible to estimate from the Monte Carlo simulations a bound on the fluctuations around the average periodic structure of each monolayer system. This provides a measure of the extent to which periodicity in these systems is well defined. The calculated fluctuations in the nearest neighbor distance are of the order of $\pm 0.2$ Å at most, and to be roughly the same for the dilute mixtures (e.g., 10% Kr:90% Xe; 10% Xe:90% Kr) and the more equally mixed systems. Thus, even the heavily mixed monolayers such as 50% Xe:50% Kr exhibit very good crystalline order. This is also in accord with the sharply defined peaks observed experimentally.[34] More quantitative comments on the sizes of the period domains and the degree of translational and orientational order in the monolayers will be given below, in Sec. III B. However, the fact that mixtures of two spherical species of different sizes and interactions can peak in periodic structures upon a flat supporting surface is of fundamental interest. The issue has received considerable attention in the context of order and disorder in two-dimensional systems.[36] The decisive factor in the stability of periodic structures over extensive domains in such systems is the similarity in the sizes of the two species involved, the size ratio being about 10:9 in the present case. This is in the spirit of the general discussion by Nelson *et al.*[36,37] However, the calculations indicate that some role is also played here by the fact that the two types of atoms are not situated at the same distance from the supporting surface plane. This reduces the packing strains.

### B. Translational and angular order

Useful insights into the structural properties of the system can be gained by examining relevant correlation functions, that can be readily constructed from the Monte Carlo simulations. We consider first the radial distribution function $g(r)$, which measures the probability density for finding an atom in the monolayer at distance $r$ from a given atom.[38] Note that we apply the definition here without a distinction as to the identity of the atoms. Figures 3(a), 3(b), and 3(c) show the calculated $g(r)$ for three monolayers at 40 K: The 10% Kr, 50% Kr, and 90% Kr systems. The structure of sharply defined peaks seen in the figures is an indication that the monolayers here have a very high degree of translational order along the surface plane. Since the variable $r$ is defined as a radial distance, the well-defined structure of $g(r)$ in Figs. 3 at least for

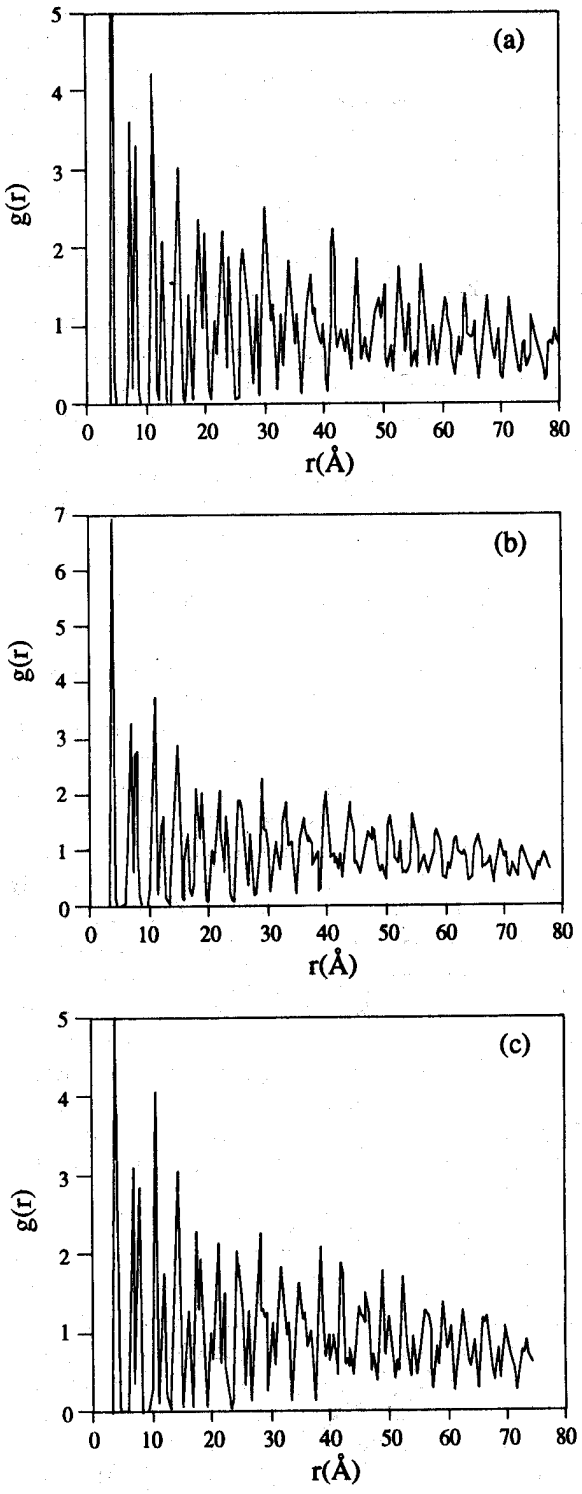


FIG. 3. Radial distribution function $g(r)$ for three Xe+Kr monolayers at 40 K: (a) 10% Kr; (b) 50% Kr; and (c) 90% Kr.

$r \lesssim 70$ Å suggests periodic domains of a linear extension of $\sim 100$ Å or more. The limited size of the simulated clusters exclude the possibility of reliable calculations of $g(r)$ at larger distances. Comparison of Figs. 3(a), 3(c) with 3(b) suggests that the 50% Xe:50% Kr may be slightly less well ordered than the cases where one of the components is

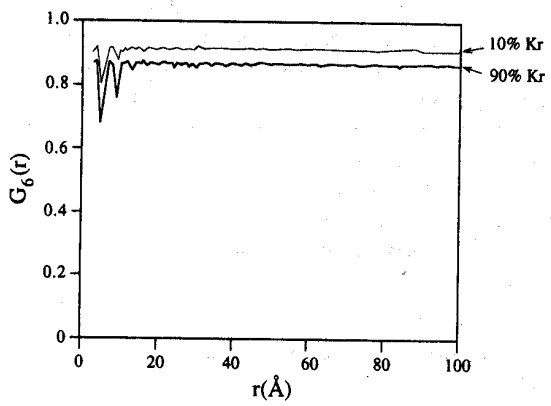


FIG. 4. Orientational correlation function $G_6(r)$ for Xe+Kr monolayers at 40 K: 10% Kr—thin line; 90% Kr—boldface line.

dilute, but the quality of crystalline-periodic order is good in all cases. This is in excellent agreement with the experimental results: The linewidth of the Bragg peaks slightly increase towards the 50% Kr:50% Xe mixture but still indicate periodically ordered structures over a length scale $>100$ Å.[34]

We now proceed to examine the orientational correlation function $G_6(r)$ for the monolayers.[36] This function, introduced by Nelson *et al.*[36,37] has been a very useful tool in analyzing long-range orientational order in surfaces of hexagonal structure.[39,40] $G_6(r)$ measures the probability density that the sixfold correlation in the orientation of nearest-neighbor atom–atom distance vectors will persist over the distance $r$. Figure 4 shows the function $G_6(r)$, calculated from the Monte Carlo simulation results, for the Xe+Kr monolayers containing 10% and 90% Kr, respectively. The fact that $G_6(r)$ in both cases remains essentially constant for $r$ values up to 100 Å means that the orientational sixfold order is maintained, and does not deteriorate at all, at least not over this distance range. (The very short range fluctuations manifested as dips are of no interest in this respect.) Again, this points to a crystal of good orientational order in domains having linear dimensions probably much larger than 100 Å. The limited sizes of the samples used in the simulations did not make it possible to explore correlations over larger distances. This result, again, is in excellent agreement with the experiment: The measured Xe+Kr monolayers Bragg peaks are azimuthally sharp and strongly correlated with the Pt(111) substrate symmetry directions. For all mixing ratios no significant azimuthal broadening of the diffraction peaks compared to those of the pure Kr and Xe components is observed, indicating a very high degree of orientational order. We note in passing that we also carried out detailed calculations and He diffraction experiments for mixed Ar+Xe monolayers, which turn out to be amorphous. For these monolayers, unlike the present case, $G_6(r)$ decays rapidly as a function of $r$, indicating short-range orientational order. The finding that $G_6(r)$ for the 10% Kr case is larger than the corresponding function for the 90% Kr monolayer can be attributed to the fact that the angular

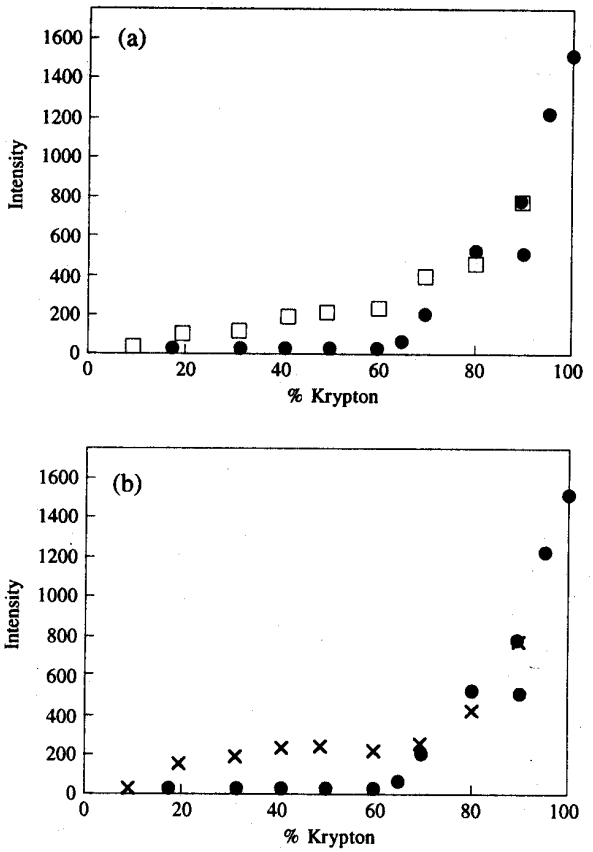


FIG. 5. Experimental and theoretical intensities of the (1,0) diffraction peak vs Xe:Kr mixing ratio. Experimental points are indicated by full circles. Multiple circles at a constant mixture concentration result from duplicate experiments. (a) □—theoretical results for a structure in which the Xe is nearer to the surface plane than Kr. (b) ×—theoretical results for the structure where the Kr atoms lie nearer to the surface plane than Xe.

structural perturbation due to a large defect in a host consisting of smaller atoms is greater due to packing considerations than in the opposite case. We conclude from the study of the correlation functions that very high translational as well as orientational order persists in all the monolayers over distances well over 100 Å.

### C. Theoretical versus experimental diffraction intensities, and the randomness of substitutional disorder

We now proceed to compare the experimental diffraction intensities for the (1,0) and (2,0) Bragg peaks, for the various Xe+Kr monolayers with the corresponding theoretical results. In making the comparison, we multiplied the results of the calculations of scattering from the static monolayers with the scaling factor of Eq. (11), which represents a Debye–Waller attenuation effect for the disordered system. Figures 5 and 6 show the comparison between the experimental and the theoretical intensities for the (1,0) and (2,0) diffraction peaks, respectively, as a function of the Xe:Kr mixing ratio of the monolayer. The theoretical intensities in Figs. 5(a) and 6(a) were com-

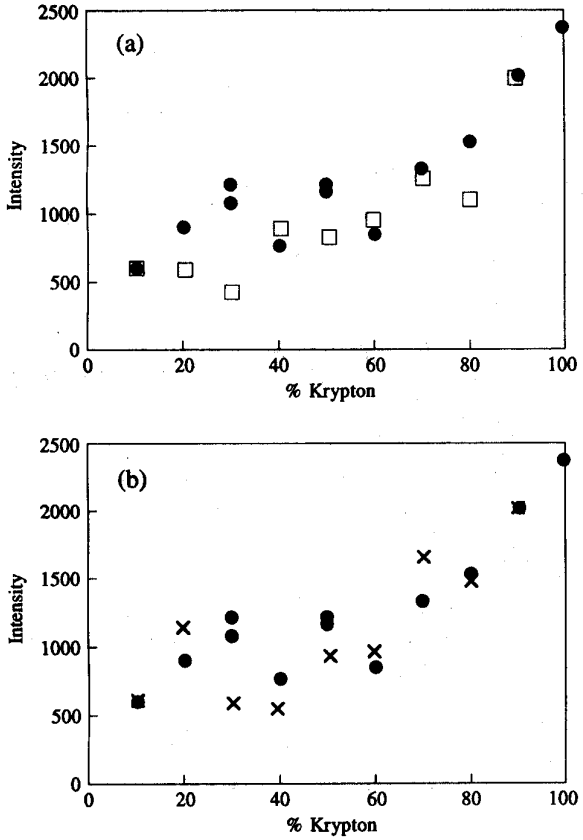


FIG. 6. Experimental and theoretical intensities of the (2,0) diffraction peak vs Xe:Kr mixing ratio. The experimental values are indicated by full circles. (a) □—theoretical results for the structure where Xe lies nearer to the surface plane than Kr. (b) ×—theoretical intensities for the structure where Kr lies nearer to Pt than Xe.

puted using the simulated structures that correspond to Xe lying closer to the Pt plane than Kr. Figures 5(b) and 6(b) again compare theory and experiment for the (1,0) and (2,0) diffraction peak, but in this case the scattering calculations were done for the structure in which the Kr atom lies nearer to the Pt plane than the Xe atom (see the discussion in Sec. II A). While there are important quantitative differences, the overall agreement between theory and experiment is good, both in Figs. 5 and 6. This shows that the theoretical structures used in the two respective calculations are at least good approximations for those structural properties to which the experiment is sensitive. The theoretical structural models corresponding to Figs. (5a), (6a) and for Figs. (5b), (6b) differ in the relative distance of the Xe and the Kr atoms from the Pt surface, but are otherwise quite similar in lateral structure, which is the property to which the experiment appears to be most sensitive.

A very important property common to the lateral structure of the models used in Figs. 5 and 6 is the nature of the substitutional disorder in the monolayers. The Monte Carlo simulations show that the substitutional disorder in these systems is almost ideally random (or stochastic), that is *the probability that any given site is occupied by a Xe or a Kr atom was found to depend to an excellent approximation only on the total Xe:Kr mixing ratio*, and is on the average independent of the identity of the neighboring atoms. A significant nonrandom propensity in the mixed monolayers would have significant effects on the lateral structure. *The agreement between the theoretical intensities (obtained from random substitutional disorder structures) and the experimental data is evidence for suggesting that the monolayers have indeed a random substitutional disorder.*

### D. Disorder rainbows: A new signature of surface disorder

As is obvious from the results of the previous subsection, the Bragg peak intensities for He scattering from periodic systems are strongly affected by substitutional disorder. Quantitative analysis of these intensities can therefore provide very useful information on the disordered structures. However, the relation between the Bragg peak intensities and the characteristic of the disorder is quite indirect. It would clearly be advantageous to have observable features that are direct signatures of the disorder. A property of this type was recently discovered in theoretical studies of He scattering from models of Xe+Kr mixed monolayers on a flat support[5]—very similar to the systems studied here except for quantitative details. The signatures found were intensity maxima at non-Bragg positions, which can therefore not arise at all for an ordered system, and thus must reflect directly the surface disorder. Examination of these maxima has shown that they can be interpreted as *rainbows*.[5,17] It can be shown by stationary-phase (classical-limit) evaluation of the intensity expression, Eq. (6), that rainbow peaks occur when the He scattering phase shifts, defined by Eq. (7), for the important configurations that contribute to the disordered structure, have an *inflection point*, i.e.,

$$\det\begin{bmatrix} \dfrac{\partial^2\eta_r(\mathbf{R})}{\partial x^2}, & \dfrac{\partial^2\eta_r(\mathbf{R})}{\partial y\,\partial x} \\ \dfrac{\partial^2\eta_r(\mathbf{R})}{\partial x\,\partial y}, & \dfrac{\partial^2\eta_r(\mathbf{R})}{\partial y^2} \end{bmatrix}=0. \tag{12}$$

The existence of an inflection point of the phase shift is related in turn to an inflection point of the He/surface potential, and the rainbow peak is due to scattering from the vicinity of that point. Rainbows have been known for He scattering from ordered surfaces[17]—in which case the observable peaks are only Bragg peaks, and the rainbow pattern is just the (semiclassical) envelope of the diffraction spikes. Rainbows were also found for scattering from isolated defects on crystalline surfaces.[29,31,17] *In the present and other cases of disordered surfaces rainbow peaks need not coincide in position with the Bragg peaks* so the two types of peaks can be readily differentiated. Since these rainbows are strictly due to disorder we refer to them as "disorder rainbows." In the example of Ref. 5, the local regions that gave rise to disorder rainbow scattering were mostly Xe atoms surrounded by Kr neighbors or vice versa. Our aim here is to explore theoretically whether

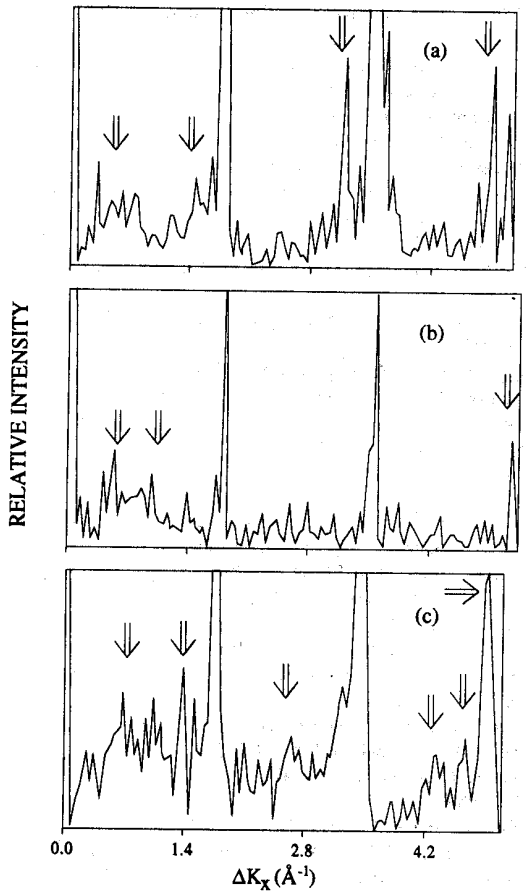


FIG. 7. Angular intensity distribution of He scattered from mixed Xe+Kr monolayers. The results are for normal incidence at He collision energy of 17.5 meV. The sharp spikes (out of scale) are the Bragg peaks. Rainbows are indicated by arrows. $\hbar\Delta K_x$ is the momentum transfer parallel to the surface along the Γ direction of the complete mixture. (a) 10% Xe:90% Kr monolayer; (b) 50% Xe:50% Kr monolayer; and (c) 90% Xe:10% Kr monolayer.

disorder rainbows also arise for the more realistic substitutionally disordered monolayers simulated in the present study. As Fig. 7 shows, this is indeed the case. In fact, as for the model study of Ref. 5, disorder rainbow maxima are found for all Xe+Kr mixed monolayers. The peak intensities and, in part, also the positions vary, however, depending on the disorder surface structures that contribute to the scattering which in turn depend on the Xe:Kr mixing ratio of the monolayer. A more detailed analysis shows that the disorder rainbow peaks for mixtures dilute in Xe come mainly from scattering from "clusters" where a Xe atom is surrounded by six Kr atoms (other clusters contribute considerably less). The rainbows for mixtures dilute in Kr come primarily from sites where a Kr atom is surrounded by six Xe's. For the heavily mixed surfaces, both types of arrangements (and probably additional ones) contribute. This feature and all the above behavior are the same as previously found in Ref. 5, for a simpler structural model of Kr+Xe overlayers. Based on the results of Fig. 7 and of Ref. 5, a search for disorder rainbows in systems such as mixed Xe+Kr monolayers should be of great interest, and may provide very detailed information on the disordered structures involved, including information on the difference between the equilibrium distances of Xe and Kr from the Pt(111) surface. The intensity of the disorder rainbows is estimated to be around $1{:}10^4$–$1{:}10^5$ as compared to the specular peak intensity in systems of this type. Experimental observation of such low intensity peaks is feasible, but hereto have not been undertaken for mixed overlayers.

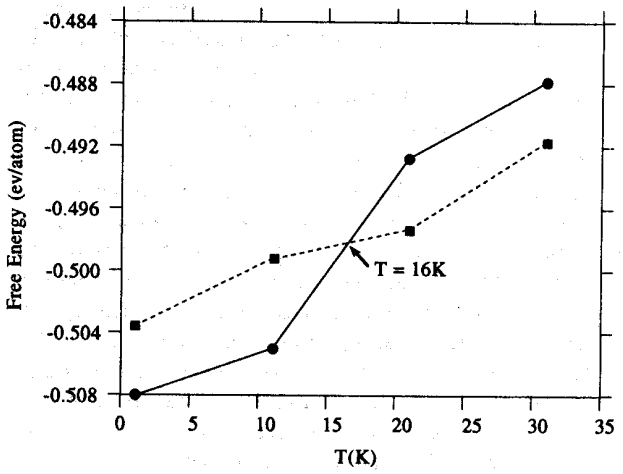


FIG. 8. Free energy curves and the segregation transition. The result is obtained for the 50% Xe:50% Kr monolayer. ●—The free energy of the mixed monolayer; □—the corresponding free energy of the segregated Xe and Kr monolayer.

### E. The segregation transition in mixed Xe+Kr monolayers

So far, our discussion was confined to structural properties only. We comment now briefly on one important thermodynamic property of these systems. Figure 8 shows the free energy curve of the mixed Xe+Kr monolayer, for a mixing ratio 1:1, and the sum of the free energies of the corresponding pure Xe and pure Kr monolayer system. The results are extracted from the Monte Carlo simulations, and are of course subject to errors due to the limited accuracy of the potentials used. The results predict a segregation transition around 16 K. If the conditions for the transition could be realized, the transition should be observable by He diffraction, since the segregated phases correspond to ordered domains of Xe and Kr monolayers. In the experiments, however, it turns out that at temperatures below about 30 K the interlayer diffusion is very small, such that kinetic effects will hinder the segregation.

## IV. CONCLUDING REMARKS

In this paper, theoretical Monte Carlo simulations and the scattering calculations from the simulated structure, and their comparison with experimental data were used to investigate the structural properties of mixed Xe+Kr monolayers.

The results have shown that under the conditions of the study, i.e., $T=40$ K, Xe+Kr mixed monolayers are crystalline periodic in structure, and have periodicity domains well over 100 Å. The lattice constants were found to depend linearly on the mixing ratios, but the periodicity was found to hold in all the regimes of mixing ratios, from dilute Xe in Kr to the opposite case, and including the heavily mixed systems. This is a first experimental–theoretical demonstration of such periodicity over the entire range of all mixing ratios in a realistic surface system of relatively well known interaction potentials. This system is therefore an ideal testing ground for models of periodicity and of angular and translational correlations in disordered surface systems. It was also found that the monolayers are almost ideal substitutionally random disordered systems. Again, there is considerable conceptual importance and interest in demonstrating such a property for systems which are real on one hand, but where relatively reliable calculations are feasible on the other hand.

Above all, this study brings out the power and potential usefulness of He diffraction scattering for exploring structural disorder at surfaces. In particular, such studies can gain much from quantitative interaction between theory and experiment. It appears that He diffraction can serve as the basis for crystallography of substitutionally disordered surfaces. This study indicates that other aspects of the scattering and its angular distribution (i.e., disorder rainbows) exist and may considerably enhance our ability to unravel disordered surface structures at great detail (on the atomic level). Further studies of related systems (e.g., mixed Ar+Xe monolayers) are under way, and will hopefully reveal different types of structural disorder in two dimensions.

## ACKNOWLEDGMENTS

This work was supported by Grant No. I-00087 from the German–Israel Foundation for Scientific Research (G.I.F.). The Fritz Haber Research Center at the Hebrew University is supported by the Minerva Gesellschaft für die Forschung mbH, Munich, Germany. The research was supported in part by the Institute of Surface and Interface Science at U.C. Irvine.

[1] See, for instance, L. W. Bruch and J. M. Phillips, Surface Sci. **91**, 1 (1980).
[2] H. Jonsson, J. G. Weare, T. H. Ellis, G. Scoles, and U. Valbusa, Phys. Rev. B **30**, 4203 (1984).
[3] K. Kern and G. Comsa, in *Phase Transitions in Surface Films*, edited by H. Taub, G. Torzo, H. J. Lauker, and S. C. Fain, Jr. (Plenum, New York, 1991), p. 41.
[4] D. K. Gibson and S. J. Sibener, J. Chem. Phys. **88**, 7862 (1988); **88**, 7893 (1988).
[5] R. B. Gerber and A. T. Yinnon, Chem. Phys. Lett. **181**, 533 (1991).
[6] K. Kern and G. Comsa, *Advances in Chemical Physics*, edited by W. P. Lawley (Wiley, New York, 1989), p. 211.
[7] J. P. Toennies, J. Vac. Sci. Technol. A **5**, 440 (1987).
[8] J. A. Barker and D. J. Auerbach, Surf. Sci. Rep. **4**, 59 (1983).
[9] B. Poelsema and G. Comsa, *Scattering of Thermal Energy Atoms from Disordered Surfaces*, Springer Tracts in Modern Physics, Vol. 115 (Springer, Berlin, 1989).
[10] A. Lahee, J. R. Manson, J.-P. Toennies, and C. Wöll, Phys. Rev. Lett. **57**, 47 (1986).
[11] A. Lahee, J. R. Manson, J.-P. Toennies, and C. Wöll, J. Chem. Phys. **86**, 7194 (1987).
[12] A. Schlup and K. H. Rieder, Phys. Rev. Lett. **56**, 73 (1985).
[13] J. Black, unpublished report, Dept. of Physics, Brock University, Ontario, Canada.
[14] J. A. Barker and C. T. Rettner, J. Chem. Phys. **97**, 5844 (1992).
[15] R. A. Aziz, in *Inert Gases*, edited by M. L. Klein (Springer-Verlag, Berlin, 1984), p. 5.
[16] *Applications of the Monte Carlo Method in Statistical Physics*, 2nd ed., edited by K. Binder (Springer-Verlag, Berlin, 1987).
[17] R. B. Gerber, Chem. Rev. **87**, 29 (1987).
[18] J. M. Hutson and C. Schwartz, J. Chem. Phys. **79**, 5179 (1983).
[19] J. R. Manson, Surf. Sci. **272**, 130 (1992).
[20] D. Hines and V. Celli, Surf. Sci. **272**, 139 (1992).
[21] R. B. Gerber, A. T. Yinnon, M. Yanuka, and D. Chase, Surf. Sci. **272**, 81 (1992).
[22] R. Spadacini and G. E. Tommei, Surf. Sci. **133**, 216 (1983).
[23] A. Kara and G. Armand, Surf. Sci. **152/153**, 77 (1985).
[24] J. I. Gersten, R. B. Gerber, D. K. Dacol, and H. Rabitz, J. Chem. Phys. **78**, 4277 (1983).
[25] G. Drolshagen and E. J. Heller, Surf. Sci. **139**, 26 (1984).
[26] A. T. Yinnon, R. Kosloff, and R. B. Gerber, Surf. Sci. **148**, 148 (1984).
[27] K. B. Whaley and A. Bennet, J. Chem. Phys. **95**, 6136 (1992).
[28] R. B. Gerber, A. T. Yinnon, and J. N. Murrell, Chem. Phys. **31**, 1 (1978).
[29] A. T. Yinnon, R. Kosloff, and R. B. Gerber, J. Chem. Phys. **88**, 7209 (1988).
[30] B. J. Hinch, Surf. Sci. **221**, 346 (1989).
[31] A. T. Yinnon, R. B. Gerber, D. K. Dacol, and H. Rabitz, J. Chem. Phys. **84**, 5955 (1986).
[32] R. David, K. Kern, P. Zeppenfeld, and G. Comsa, Rev. Sci. Instrum. **57**, 2771 (1986).
[33] C. H. Hsu, B. E. Larson, M. El-Batanauny, C. R. Willis, and K. M. Martin, Phys. Rev. Lett. **66**, 3164 (1991).
[34] P. Zeppenfeld, K. Kern, R. David, U. Becher, and G. Comsa, Surf. Sci. Lett. **285**, L461 (1993).
[35] A. R. West, *Solid State Chemistry and its Applications* (Wiley, Chichester, England, 1984).
[36] D. R. Nelson, M. Rubinstein, and F. Speapen, Philos. Mag. A **46**, 105 (1982).
[37] D. R. Nelson and B. I. Halperin, Phys. Rev. B **19**, 2457 (1979).
[38] D. A. McQuarrie, *Statistical Mechanics* (Harper and Row, New York, 1976).
[39] C. A. Murray, W. O. Sprenger, and R. A. Wenk, Phys. Rev. B **42**, 688 (1990).
[40] H. Dai, H. Chen, and C. M. Leiber, Phys. Rev. Lett. **66**, 3183 (1991).